

# Oxidation behaviour of carbon short fibre reinforced C/SiC composites

Friedrich Raether<sup>a,\*</sup>, Jürgen Meinhardt<sup>a</sup>, Andreas Kienzle<sup>b</sup>

<sup>a</sup> *Fraunhofer-Institut ISC, Neunerplatz, D-97082 Würzburg, Germany*

<sup>b</sup> *SGL Carbon GmbH, Werner-von-Siemens-Str. 18, D-86405 Meitingen, Germany*

Available online 8 June 2006

## Abstract

Oxidation kinetics of carbon short fibre reinforced C/SiC composites was measured by a thermobalance. The oxidation along the carbon fibre bundles and their contacts was identified as the dominating mechanism. To improve oxidation resistance, oxidation barriers in the junctions between the fibre bundles have to be established. Therefore, the infiltration of the carbon prepregs by molten silicon, which is essential for the formation of microstructure during the production of the composites, was investigated. The infiltration was monitored in situ using a thermo-optical measuring device (TOM). Infiltration kinetics was controlled by SiC formation at a temperature below 1500 °C and by capillary flow at a temperature of 1700 °C.

© 2006 Elsevier Ltd. All rights reserved.

**Keywords:** Composites; Corrosion; Carbides; Wear parts

## 1. Introduction

C/SiC composites have an excellent fracture toughness. For future applications composites are required which have long-term oxidation resistance at high temperatures and can simultaneously withstand high mechanical loads. No carbon fibre reinforced ceramics exist until now which possess long-term oxidation resistance without an external oxidation barrier at temperatures higher than 500 °C.<sup>1–6</sup> Future applications like brake disks for heavy vehicles, e.g. trucks and trains, require exactly this property because it is not possible to protect the friction surface with an oxidation protecting coating. For lighter vehicles like passenger cars, brake disks made of carbon fibre reinforced SiC ceramics are already produced.<sup>7,8</sup> They last for more than 300,000 km which is above the life time of most passenger cars. As usual the C/SiC ceramics are produced from porous preforms of carbon fibres which are bound by low-density carbon. These C/C preforms are infiltrated by liquid silicon (LSI<sup>9,10</sup>) which reacts with the low-density carbon to form SiC. The advantage of the novel C/SiC ceramic is the use of short fibres bundles instead of the conventionally used long fibres.<sup>11</sup> Short fibres allow the development of an inner oxidation protection. In this case only the short fibre bundles which have direct contact to the surface of the brake disks oxidise, whereas the inner short

fibres are protected by the matrix. The short fibre bundles are produced from long carbon fibres by adding resins as binder, pyrolysis giving the low-density carbon binder and chopping of the filaments.

One problem preventing such an inner oxidation protection in C/SiC ceramics could be the network of microcracks which results from the mismatch of thermal expansion between the carbon fibre bundles and the SiC matrix during cooling after the LSI process.<sup>9</sup> Microcracks between the short fibre bundles open diffusion paths for oxygen to the inner bundles. Further diffusion paths could be junctions between the short fibre bundles. The paper presents results from a joint project which aims at a better understanding of the relation between processing, microstructure and oxidation behaviour by using in situ measuring methods for monitoring infiltration and oxidation of the C/SiC composites.

## 2. Experimental

Most experiments were performed using cube shaped C/SiC or C/C samples with an edge length of 30 mm. These samples were prepared from large compacts by sawing, grinding and polishing with a diamond saw, diamond paper and diamond suspension, respectively. In this way for the C/SiC samples short fibre bundles were cut off at the surface of the cubes and only inner bundles were protected by the matrix. The composition of standard C/SiC samples was 30 wt% carbon, 60 wt% SiC and 10 wt% Si. The liquid silicon infiltration into the C/C samples

\* Corresponding author.

E-mail address: [raether@isc.fraunhofer.de](mailto:raether@isc.fraunhofer.de) (F. Raether).

and the oxidation of the C/SiC samples were investigated using in-house built thermo-optical measuring devices: TOM. These devices enable a simultaneous in situ measurement of changes of sample shape, mass and heat transfer during heat treatments in various atmospheres.<sup>12</sup>

Liquid silicon was infiltrated in vacuum after melting the Si in a carbon crucible within a graphite furnace. The C/C sample was preheated to the same temperature in the same furnace by suspending it some centimetres above the silicon melt. Then the C/C sample was lowered until it had contact to three porous carbon stilts which were placed within the melt. There was no direct contact between the C/C sample and the melt and the infiltration occurred only via the carbon stilts. The infiltration frontier was measured by an optical dimension measuring system. Different emissivities of Si and C during the infiltration provided a sufficient optical contrast to measure the vertical position of the borderline between the infiltrated and not infiltrated region of the sample. Accuracy of position measurement was  $\pm 1$  mm.

Weight changes during corrosion of the C/SiC cubes were measured at constant temperatures between 500 °C and 1300 °C in ambient air in a MoSi<sub>2</sub> resistance heated furnace. The samples were suspended from a commercial balance above the furnace. A drift of the balance was eliminated by carefully stabilising its temperature. Accuracy of weight measurement was 0.02%. The C/SiC samples were heated with a heating rate of 5 °C/min to the holding temperature. (Due to oxidation during the heating period a weight loss up to 4% occurred before the isothermal measurements were started.) Also single short fibre bundles were investigated using customary thermogravimetry (SETARAM TAG 24). Those fibre bundles had a length of 10 mm, a width of 2 mm and a height of 0.8 mm. They were measured at constant temperatures in synthetic air (flow rate 1 l/h). The microstructure investigation was performed with a scanning electron microscope LEO 1450VP.

### 3. Results and discussion

Fig. 1 shows the infiltration of the liquid silicon into the porous C/C preform at 1485 °C and 1700 °C. (The melting point of silicon is at 1420 °C.) Whereas infiltration depth was proportional to infiltration time at 1485 °C, it was proportional to the square root of the infiltration time at 1700 °C (compare solid lines in Fig. 1).

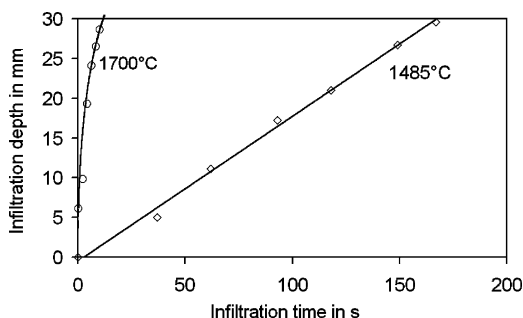


Fig. 1. Silicon infiltration depth at 1485 °C and 1700 °C (open symbols) showing square root and linear dependence, respectively (solid lines).

The infiltration of porous bodies is described by the well known Washburn equation<sup>13</sup>:

$$x^2 = \left( \frac{\gamma \cdot \cos \Theta}{2 \cdot \eta} \right) \cdot r \cdot t, \quad (1)$$

where  $x$ : infiltration depth,  $r$ : pore radius,  $t$ : infiltration time,  $\eta$ : viscosity,  $\gamma$ : surface tension and  $\Theta$ : contact angle. The term in brackets is the so-called penetration coefficient. Comparing the infiltration curves in Fig. 1 the infiltration at 1700 °C is about 12 times faster than at 1485 °C. Because the porosity and the average radius of the pores of the C/C preform were the same in both experiments, the difference in the infiltration rate can solely result from the different penetration coefficients. The viscosity of molten silicon decreases only by a factor of 1.3 between 1485 °C and 1700 °C<sup>14</sup> and cannot explain the higher infiltration rate at 1700 °C. The changes of surface tension and contact angle also cannot explain it: surface tension decreases between 1485 °C and 1650 °C by about 10%<sup>15,16</sup> and the contact angle usually decreases slowly with temperature, too. The solubility of carbon in silicon increases from 0.01 atom% to 0.08 atom% between 1485 °C and 1700 °C<sup>17</sup> but this does not change the contact angle.<sup>18</sup>

However, silicon reacts with carbon during infiltration and forms solid SiC. This drastically improves wetting behaviour<sup>15</sup> behind the infiltration front. Considering the experimental results (Fig. 1) it was concluded that infiltration kinetics at 1485 °C was controlled by the formation of SiC, whereas at 1700 °C SiC formation was much faster and infiltration kinetics was controlled by the Washburn equation. Apparently SiC formation was not so fast that infiltration was slowed down by the narrowing of pore channels.

Fig. 2 shows the weight loss during oxidation of carbon short fibre bundles and of C/SiC samples at different temperatures.

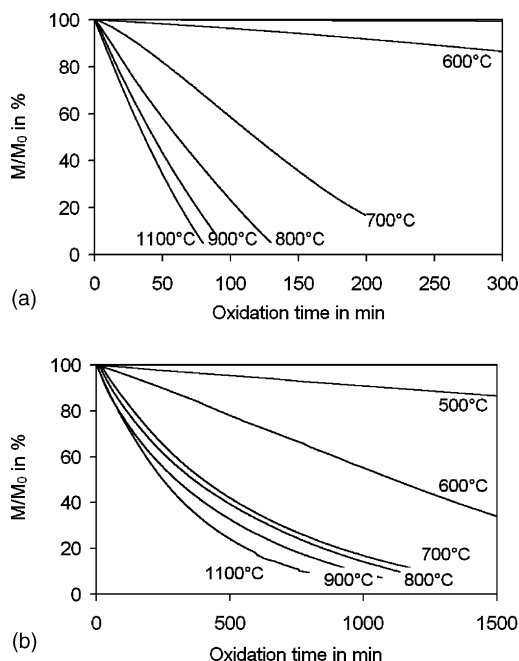


Fig. 2. Dependence of the weight loss of carbon on the oxidation time at different temperatures: (a) carbon short fibre bundles and (b) carbon in the C/SiC samples.

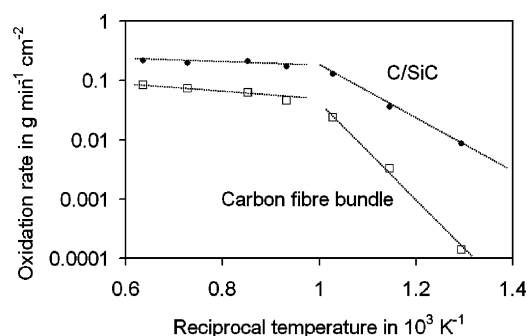


Fig. 3. Oxidation rates of the carbon short fibre reinforced SiC ceramic and of single carbon short fibre bundles: measured values (symbols) and Arrhenius curves (dotted lines).

Data were scaled by the initial carbon mass  $M_0$  of the samples. A strong increase of weight loss with temperature was observed. Whereas a linear weight loss was measured for the single fibre bundles (Fig. 2a), the weight loss rate of C/SiC samples decreased at longer oxidation times and at temperatures above 700 °C (Fig. 2b). This was attributed to the protection of the carbon fibre bundles by the matrix in the C/SiC samples: after oxidation of the exposed bundles at the cube's surface, further oxidation required diffusion of oxygen to the reaction front and transfer of the arising CO or CO<sub>2</sub> to the outside of the sample. This slowed down oxidation when the reaction rate at the carbon interface was high – at high temperatures – and the diffusion path was long—after prolonged oxidation.

An initial oxidation rate was determined by calculating the average slope of the curves in Fig. 2 between 5 mass% and 10 mass% loss. It was scaled with the initial carbon surface of the respective samples. Fig. 3 shows these oxidation rates in an Arrhenius type diagram. There were two temperature regimes above and below 730 °C which had constant activation energy for both types of samples: carbon fibre bundles and C/SiC. The activation energies were 5 kJ/mol for C/SiC and 10 kJ/mol for carbon fibre bundles in the high temperature regime and 84 kJ/mol (C/SiC) and 164 kJ/mol (carbon fibre bundles) in the low temperature regime, respectively. Two different activation energies for the oxidation of carbon were already identified and were attributed to a reaction kinetics which is controlled by the interface reaction of oxygen with carbon in the low temperature regime and the diffusion of oxygen to the interface in the high temperature regime.<sup>19–23</sup>

The smaller oxidation rates of the carbon fibre bundles compared to the C/SiC samples (Fig. 3) were in disagreement to the protecting effect of the C/SiC matrix. An explanation of this phenomenon was obtained by investigating partially oxidised C/SiC samples in the SEM (Fig. 4). It can be seen that the carbon fibres stick out of the low-density carbon matrix, i.e. their oxidation was much slower than the oxidation of the carbon matrix. This led to a steep increase of the exposed carbon surface during oxidation. Since the initial specific surface of the C/SiC samples was much smaller than that of the single fibre bundles the relative increase of surface due to the preferential oxidation of the carbon matrix was much larger resulting in seemingly larger oxidation rates. Therefore, the slope of the oxidation rates of

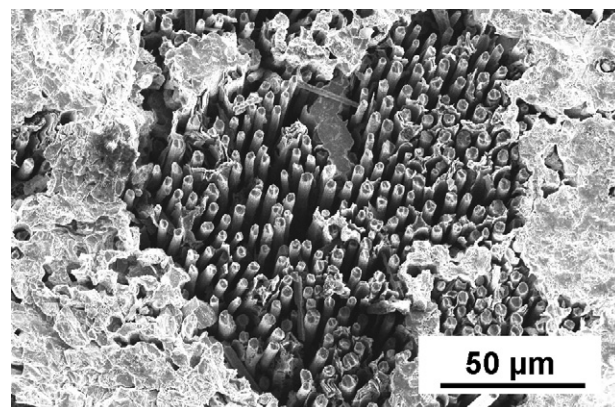


Fig. 4. SEM image of a carbon short fibre bundle in a partially oxidised C/SiC sample (the surface was exposed to oxygen).

the C/SiC samples in the Arrhenius diagram (Fig. 3) reflects a mixture of the activation energy of the local oxidation reactions and geometric changes. The differences between the two sample types decreased at higher temperatures (Fig. 3) which is consistent with the SEM observations showing smoother surfaces within the fibre bundles at higher oxidation temperatures due to enhanced oxidation of the carbon fibres.

The effect of the matrix was investigated in more detail by oxidising C/SiC cubes which were coated with an oxidation protective layer at five of its six side faces. Fig. 5 shows the comparison between the oxidation of a cube where the uncoated face was parallel to the pressing direction of the C/C preform and a cube where it was perpendicular (measured at 900 °C). The oxidation rate perpendicular to the pressing direction was twice as much as the rate parallel to the pressing direction. This was explained by a preferred orientation of the fibre bundles perpendicular to the pressing direction (Fig. 6).

The orientation of the microcracks in the C/SiC samples (not visible in Fig. 6) was perpendicular to the fibre bundles, i.e. mainly parallel to the pressing direction. The reason is the well known anisotropic stress caused by mismatch of thermal expansion between fibre bundles and matrix during cooling of the samples after the LSI process. Therefore, oxidation via the microcracks would have led to a preferred oxidation in pressing direction. On the other hand, due to the anisotropy of fibre orientation, oxidation via the fibre bundles and its contacts required a longer zigzag-path parallel to the pressing direction than perpen-

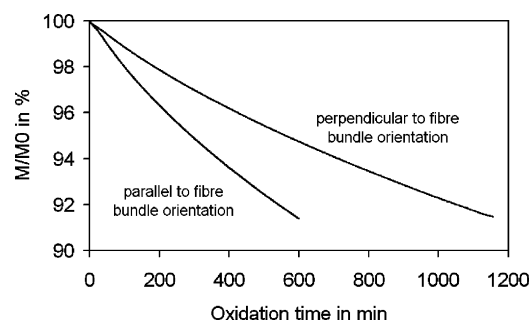


Fig. 5. Dependence of the weight loss on the oxidation time of a C/SiC sample corroded parallel and perpendicular to the bundle orientation, respectively.



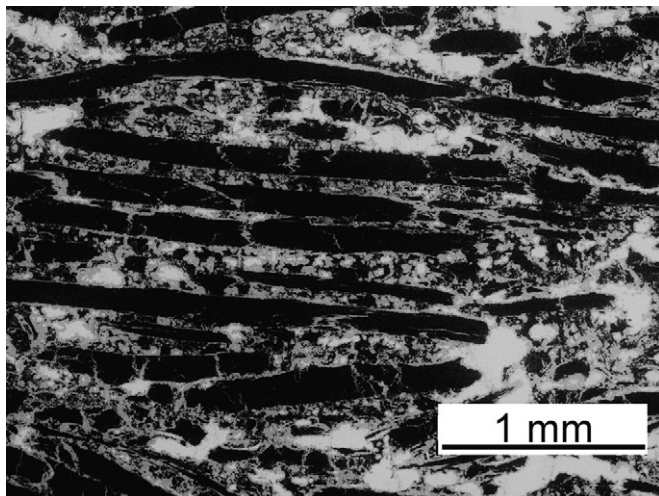


Fig. 6. Back scattered electron SEM image of a polished section of a C/SiC sample (black: carbon; grey: SiC; white: Si).

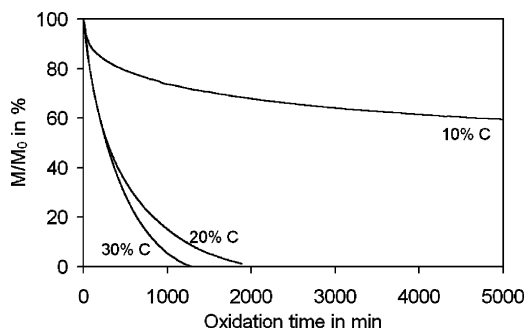


Fig. 7. Oxidation of C/SiC samples with different total carbon contents: (a) 30 wt%; (b) 20 wt%; (c) 10 wt%.

pendicular to it. Therefore, it was concluded that oxidation via the contacts between the fibre bundles was the dominating mechanism.

Fig. 7 shows the oxidation behaviour of differently processed C/SiC samples resulting in varying carbon concentrations. The contacts between the carbon fibre bundles were strongly reduced by decreasing their fraction from the standard sample with 30 wt% carbon to the sample with 20 wt% and 10 wt% carbon. A significant reduction of oxidation rate was observed by this procedure which cannot be explained by the reduced percolation of the fibre bundles due to their decreasing volume fraction alone. Note that the data were scaled by the initial carbon content  $M_0$ .

#### 4. Conclusions

For the first time liquid silicon infiltration into a C/C preform has been investigated in situ. The results show a change of the infiltration mechanism from a linear time dependence to a square root time dependence by increasing the infiltration temperature from 1485 °C to 1700 °C. It was also the first time that the oxidation behaviour of a carbon short fibre reinforced SiC composite was investigated. The composite oxidises along the short fibre bundles and their contacts. The effect of the microcracks on the oxidation behaviour is negligible. Further development aims at

increasing the carbon short fibre bundle content simultaneously to the reduction of bundle contacts.

#### Acknowledgements

The authors thank the Bayerische Forschungsförderung für finanzielle Unterstützung innerhalb des gemeinsamen Forschungsprojekts "Werkstoffe auf Basis von Kohlenstoff" (FORCARBON) und C. Hermann und I. Krätschmer für Hilfe bei den Messungen und der Probenherstellung.

#### References

1. Bacos, M.-P. and Sudre, O., Critical review on oxidation protection for carbon-based composites. *Ceram. Trans./High-Temp. Ceram.-Matrix Compos.*, 1995, **57/I**, 437–442.
2. Westwood, M. E., Webster, J. D., Day, R. J., Hayes, F. H. and Taylor, R., Review—oxidation protection for carbon fibre composites. *J. Mater. Sci.*, 1996, **31**, 1389–1397.
3. Labanti, M., Martignani, G., Mingazzini, C., Minocari, G. L., Pilotti, L., Ricci, A. and Weiss, R., Evaluation of damage by oxidation corrosion at high temperatures of coated C/C–SiC ceramic composite. High Temperature Ceramic Matrix Composites. 4th International Conference on high Temperature Ceramic Matrix Composites, Oct. 1–3, 2001, Munich, Germany, 2001, pp. 218–223.
4. Wunder, V., Popovska, N. and Emig, G., Oxidation-resistant coatings on C/C and C/SiC composites by chemical vapor deposition (CVD). Werkstoffwoche '98, Band VII: Symposium 9, Keramik; Symposium 14, Simulation Keramik, Sept., 1998, Munich, 1999, Meeting Date 1998, pp. 515–520.
5. Haug, R., Heimann, D., Bill, J. and Aldinger, F., Ceramic oxidation-resistant coatings from polymer precursors. Verbundwerkstoffe und Werkstoffverbunde, [Vortragstexte der Tagung], Bayreuth, Oct. 24–25, 1995, Germany, 1996, Meeting Date 1995, 429–432.
6. Ullmann, T., Schmücker, M., Hald, H., Henne, R. and Schneider, H., Yttrium-silicates for oxidation protection of C/C–SiC composites. High Temperature Ceramic Matrix Composites, [4th International Conference on High Temperature Ceramic Matrix Composites], Oct. 1–3, 2001, Munich, Germany, 2001, pp. 230–235.
7. Gruber, U., Heine, M. and Kienzle, A., Mit Fasern und/oder Faserbündeln verstärkter Verbundwerkstoff mit keramischer Matrix, Offenlegungsschrift DE 199 44 345 A 1 vom 16.9.1999.
8. Heine, M. and Gruber, U., Mit Graphitfasern verstärkter Siliziumcarbidkörper, Offenlegungsschrift DE 197 10 105 A 1 vom 12.3.1997.
9. Gern, F. and Kochendörfer, R., Liquid silicon infiltration: description of infiltration dynamics and silicon carbide formation. *Compos.: Part A Appl. Sci. Manuf.*, 1997, **28A**(4), 335–364.
10. Krenkel, W., Verfahren zur Herstellung eines mit Kohlenstoff-Fasern verstärkten, keramisierten Formkörpers und Verwendung eines solchen Formkörpers, Patentschrift DE 197 49 462 C 1 vom 10.11.1997.
11. Papenburg, U., Blenninger, E., Kunkel, B. and Deyerler, M., Optomechanische Leichtgewichtsstrukturen aus kurzfaserverstärkter Keramik, Fortschrittsberichte DKG. In Seminar "Festigkeit Keramischer (Verbund-)Werkstoffe", 1994, pp. 1–43.
12. Baber, J., Klimera, A. and Raether, F., In situ measurement of dimensional changes and temperature fields during sintering with a novel thermo-optical measuring device. *J. Eur. Ceram. Soc.*, submitted for publication.
13. Adamson, A. W., *Physical Chemistry of Surfaces*. John Wiley & Sons, New York, 1990.
14. Brooks, R. F., Dinsdale, A. T. and Quested, P. N., The measurement of viscosity of alloys—a review of methods, data and models. *Meas. Sci. Technol.*, 2005, **16**, 354–362.
15. Li, J.-G. and Hausner, H., Wetting and adhesion in liquid silicon/ceramic systems. *Mater. Lett.*, 1992, **14**, 329–332.
16. Li, J.-G. and Hausner, H., Wetting in reactive metal/ceramic systems, Abschlußbericht zum DFG-Forschungsvorhaben Ha 995. Technische Uni-

- versität Berlin, Institut für Nichtmetallische Werkstoffe, Germany, 26 January 1994.
17. Scace, R. I. and Slack, G. A., Solubility of carbon in silicon and germanium. *J. Chem. Phys.*, 1959, **30**(6), 1551–1555.
  18. Li, J.-G. and Hausner, H., Reactive wetting in the liquid-silicon/solid-carbon system. *J. Am. Ceram. Soc.*, 1996, **79**(4), 873–880.
  19. Lewis, J. B., Thermal gas reactions of graphite. In *Modern Aspects of Graphite Technology*, ed. L. C. F. Blackman. Academic Press, London/New York, 1970.
  20. Marsh, H. and Kuo, K., Kinetics and catalysis of carbon gasification. In *Introduction to Carbon Science*, ed. Harry Marsh. Butterworth & Co. Ltd., 1989, pp. 107–151.
  21. Walker Jr., P. L., Rusinko Jr., F. and Austin, L. G., Gas reactions of carbon. In *Advances in Catalysis and Related Subjects, Vol. XI*, ed. D. D. Eley, P. W. Selwood and P. B. Weisz. Academic Press Inc., New York/London, 1959, pp. 133–221.
  22. Rossberg, M., Experimentelle Ergebnisse über die Primärreaktionen bei der Kohlenstoffverbrennung. *Z. Elektrochem., Bd.*, 1956, **60**(9/10), 952–956.
  23. Rossberg, M. and Wicke, E., Transportvorgänge und Oberflächenreaktionen bei der Verbrennung graphitischen Kohlenstoffs. *ChemieIng.-Techn. Jahrgang*, 1956, **28**(3), 181–189.